

Robust Precoder Design for 3D Massive MIMO Downlink with A Posteriori Channel Model

An-An Lu, *Member, IEEE*, Xiqi Gao, *Fellow, IEEE* and Chengshan Xiao, *Fellow, IEEE*

Abstract

In this paper, we investigate the robust linear precoder design for three dimensional (3D) massive multi-input multi-output (MIMO) downlink with uniform planar array (UPA) and imperfect channel state information (CSI). In practical massive MIMO with UPAs, the number of antennas in each column or row is usually limited. The straightforward extension of the conventional DFT based beam domain channel model widely used in massive MIMO with uniform linear arrays (ULAs) can not apply. To overcome this issue, we establish a new beam domain channel model by using sampled steering vectors. Then, a novel method to obtain the beam domain channel power matrices and the instantaneous beam domain channel coefficients is proposed, and an *a posteriori* beam domain channel model which includes the channel aging and the spatial correlation is established. On the basis of the *a posteriori* channel model, we consider the robust precoder design with the expected weighted sum-rate maximization under a total power constraint. By viewing the power constraint as a Riemannian manifold, we transform the constrained optimization problem into an unconstrained optimization problem on the Riemannian manifold. Then, we derive an iterative algorithm to obtain the optimal precoders by setting the Riemannian gradient of the objective function to zero. Furthermore, we propose a low complexity robust precoder design by replacing the expected rates in the objective function with their upper bounds. Simulation results show that the proposed precoders can achieve significant performance gain than the widely used regularized zero forcing (RZF) precoder and signal to leakage noise ratio (SLNR) precoder.

Index Terms

3D massive multi-input multi-output (MIMO), uniform planar array (UPA), beam domain channel model, sampled steering vectors, robust linear precoders, imperfect CSI.

A.-A. Lu and X. Q. Gao are with the National Mobile Communications Research Laboratory (NCRL), Southeast University, Nanjing, 210096 China, and also with Purple Mountain Laboratories, Nanjing 211111, China, e-mail: aalu@seu.edu.cn, xqgao@seu.edu.cn.

C. Xiao is with the Department of Electrical and Computer Engineering, Lehigh University, Bethlehem, PA 18015. Email: xiaoc@lehigh.edu.

I. INTRODUCTION

Massive multiple-input multiple-output (MIMO) [1]–[4] is one of the enabling technologies of the fifth generation (5G) mobile networks. It provides enormous potential capacity gains by employing a large antenna array at a base station (BS), and enhances multi-user MIMO (MU-MIMO) transmissions on the same time and frequency resource significantly. With massive antenna arrays at the BS, it is also possible to achieve high energy efficiency. Furthermore, massive MIMO is a key technology for many new applications and services. For example, it improves the reliability and the throughput performance for communication with unmanned aerial vehicles (UAVs) [5], [6], and well suites for mass connectivity which is very important to support internet of things (IoT) [7]. There are several types of antenna array in massive MIMO systems. Among them, the uniform planar array (UPA) is a good antenna solution for practical wireless communication systems due to its compact size and three dimensional (3D) coverage ability. In this paper, we investigate the transmission for massive MIMO downlinks with UPA.

To alleviate the multi-user interference and improve the sum-rate performance, the precoders for massive MIMO downlink should be properly designed. Massive MIMO can be viewed as an extension of conventional multi-user MIMO. The precoder design for the conventional MU-MIMO and massive MIMO has been widely investigated in different forms over the past years [8]–[21]. The precoders fall into two categories: nonlinear precoders and linear precoders. The nonlinear precoders such as DPC [10] can achieve optimal performance, but their complexity is very high and thus not suitable to massive MIMO. Thus, we focus on linear precoder designs for massive MIMO in this paper. The precoder designs often depend on the available channel state information (CSI) at the BS. If the BS knows perfect CSI of all user equipments (UEs), the regularized zero forcing (RZF) precoder [9] and the signal to leakage noise ratio (SLNR) precoder [11] are widely used. Furthermore, the classic iterative weighted minimum mean square error (WMMSE) precoder [13], [15] is designed according to the sum-rate maximization criterion.

In practical massive MIMO systems, perfect CSI at the BS are usually not available due to channel estimation error, channel aging, etc. Furthermore, different user usually has different moving speeds. Thus, we model the channel uncertainty first. In the literature [14], [20], [22], [23], the channel uncertainty are often constructed as a complex Gaussian random matrix with independent and identically distributed (i.i.d.), zero mean and unit variance entries. However, the uncertainty in practical systems usually deviate from the i.i.d. assumption. To describe the

channel in practical systems more precisely, a more realistic channel model which consider the impacts of channel estimation, use the jointly correlated channel model to represent the spatial correlation, and the widely used Gauss-Markov process [24]–[26] to model the time evolution of the channel, is proposed in [27]. Following [27], we model the *a posteriori* CSI for each user as statistical CSI under a jointly correlated channel model with both channel mean and channel covariance information.

In [27], the considered massive MIMO is equipped with a large uniform linear array (ULA). For massive MIMO with ULA equipped at the BS, the DFT matrix is asymptotically the eigenmatrix for the channel covariance matrix at the BS side. Thus, the jointly correlated channel model [28]–[30] with the DFT matrix being the eigenmatrix at the BS side is widely used in the massive MIMO literature. The model is also known as the beam domain channel model as each column vector of the DFT matrix represents a spatial beam physically [18], [28]. For massive MIMO with UPA, a natural solution seems to be the Kronecker product extension of the DFT based beam domain channel representation. However, for practical massive MIMO with UPA, the number of the antennas at each column or each row is usually limited. Thus, the deviation of the DFT based channel model from the physical channel might be too large.

To obtain a more accurate channel model for the considered massive MIMO with UPA, we establish a beam domain channel model by using the matrices of sampled steering vectors, which serves as an *a priori* jointly correlated channel model. To guarantee the accuracy of the established model, the number of sampled steering vectors can be larger than the number of antennas. Furthermore, we provide a method to obtain the statistical channel power matrices and the instantaneous beam domain channel coefficients. Then, we establish an *a posteriori* beam domain channel model with both channel mean and channel covariances information. With the established *a posteriori* channel model, we are able to describe the spatial correlation and the channel uncertainty for massive MIMO with UPA more precisely. On this basis, we investigate the robust precoder design for massive MIMO downlink transmission with UPA and imperfect CSI at the BS. We consider the problem of maximizing the expected weighted sum-rate under a total power constraint, which can be viewed as a Riemannian manifold. Then, we transform the constrained optimization problem into an unconstrained one on the Riemannian manifold. By applying the optimal necessary conditions on the Riemannian manifold, we derive an iterative algorithm to obtain the robust precoder design. Further, we propose a low complexity robust precoder design by replacing the expected rates in the objective function with their upper bounds.

The rest of this article is organized as follows. The channel model is presented in Section II. The designs of robust linear precoders are shown in Section III. Simulation results are provided in Section IV. The conclusion is drawn in Section V.

Notations: Throughout this paper, uppercase and lowercase boldface letters are used for matrices and vectors, respectively. The superscripts $(\cdot)^*$, $(\cdot)^T$ and $(\cdot)^H$ denote the conjugate, transpose and conjugate transpose operations, respectively. $\mathbb{E}\{\cdot\}$ denotes the mathematical expectation operator. In some cases, where it is not clear, subscripts will be employed to emphasize the definition. The operators $\text{tr}(\cdot)$ and $\det(\cdot)$ represent the matrix trace and determinant, respectively. The operator \otimes denotes the Kronecker product. The Hadamard product of two matrices \mathbf{A} and \mathbf{B} of the same dimension is represented by $\mathbf{A} \odot \mathbf{B}$. The $N \times N$ identity matrix is denoted by \mathbf{I}_N .

II. CHANNEL MODEL

In this section, we first establish a new beam domain channel model based on sampled steering vectors as an *a priori* channel model. The new channel model generalizes the existing beam domain channel model for ULA to URA with guaranteed accuracy. We then provide a method to obtain the channel power matrix and the instantaneous beam domain channel coefficients. Finally, we build an *a posteriori* beam domain channel model with both channel mean and channel variances.

A. System Configuration

In this subsection, we introduce the system configuration of a 3D massive MIMO system with UPAs equipped in the BS. We consider a massive MIMO system with block flat fading channels. The massive MIMO system consists of one BS and K UEs. The BS is equipped with an $M_z \times M_x$ UPA of antennas, where M_z and M_x are the numbers of pairs of antennas at each vertical column and horizontal row, respectively. Thus, the number of antennas at the BS is $M_t = M_z M_x$. For simplicity, we assume that all UEs are equipped with M_k antennas which are placed in a uniform linear array (ULA). We divide the time resources into slots and each time slot contains N_b blocks, and assume the channel coefficients remain constant in a block. We focus on the case where the massive MIMO system operates in time division duplexing (TDD) mode. For simplicity, we assume that there only exists the uplink training phase and the downlink transmission phase. At each slot, the uplink training sequences are sent once at the

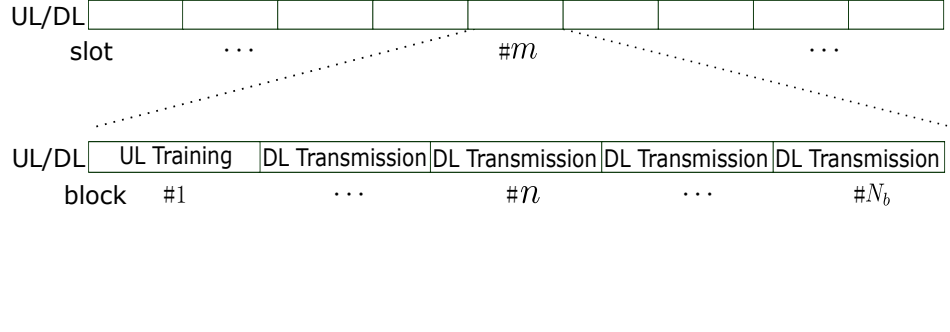


Fig. 1. Time slot structure.

first block. Furthermore, the obtained channel state information are used in the next slot. The second block to the N_b -th block are used for downlink transmission. For illustration purpose, we plot the time slot structure in Fig. 1.

B. New Beam Domain Channel Model with Sampled Steering Vectors

In this subsection, we establish a new beam domain *a priori* channel model. We denote by \mathbf{H}_{km} the channel matrix from the BS to the k -th UE at the n th block of slot m . Let θ_r denote the angle of arrival at the user side and θ_t, ϕ_t denote the polar and azimuthal angles of departure at the BS. The steering vector $\mathbf{a}_r(u_r) \in \mathbb{C}^{M_k \times 1}$ at the user side is given by

$$\mathbf{a}_r(u_r) = \frac{1}{\sqrt{M_k}} [1 \quad e^{-j2\pi\Delta_r u_r} \quad \dots \quad e^{-(M_k-1)j2\pi\Delta_r u_r}]^T \quad (1)$$

where u_r is the directional cosine with respect to the receive antenna array as $u_r = \cos\theta_t$ and $\Delta_r = \frac{d_r}{\lambda}$. For the BS, we assume there exist a 3D coordinate as plotted in Fig. 2. The UPA is put on the xz -plane. The steering vector $\mathbf{a}_t(u_t, v_t)$ for the UPA at the BS side is extended from the steering vector for the ULA as

$$\mathbf{a}_t(u_t, v_t) = \mathbf{v}_x(u_t) \otimes \mathbf{v}_z(v_t) \quad (2)$$

where

$$\mathbf{v}_z(u_t) = \frac{1}{\sqrt{M_z}} [1 \quad e^{-j2\pi\Delta_z u_t} \quad \dots \quad e^{-(M_z-1)j2\pi\Delta_z u_t}]^T \quad (3)$$

$$\mathbf{v}_x(v_t) = \frac{1}{\sqrt{M_x}} [1 \quad e^{-j2\pi\Delta_x v_t} \quad \dots \quad e^{-(M_x-1)j2\pi\Delta_x v_t}]^T \quad (4)$$

$\Delta_z = \frac{d_z}{\lambda}$, $\Delta_x = \frac{d_x}{\lambda}$, and u_t and v_t are the directional cosines with respect to the z axis and x axis, respectively, *i.e.*, we have $u_t = \cos\theta_t$ and $v_t = \sin\theta_t \cos\phi_t$. In this paper, we assume that both d_z and d_x equal 0.5λ . Then, we obtain $\Delta_z = \Delta_x = \frac{1}{2}$.

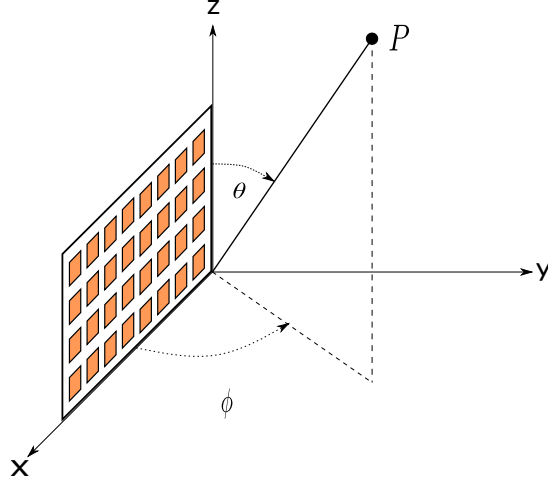


Fig. 2. 3D Coordinate.

The multipath wireless MIMO channel from the BS to the k -th user can be represented as

$$\mathbf{H}_{km} = \sum_{u_r, u_t, v_t \in \mathcal{B}_d} g_k(u_r, u_t, v_t) \mathbf{a}_r(u_r) \mathbf{a}_t(u_t, v_t)^H \quad (5)$$

where \mathcal{B}_d is the set of directional cosines corresponding to the multiple wireless paths and $g_k(u_r, u_t, v_t)$ is the fading coefficient of each path. However, the channel coefficients and the set \mathcal{B}_d in (5) are hard to obtain in practice since there are infinitely many possible u_r, u_t, v_t . To be a realistic channel model that can be used in practical systems, we discretize the possible directional cosines. Let \mathcal{B} be the set of all possible directional cosines. We partition the set \mathcal{B} into the sets $\mathcal{B}_{r,i} \times \mathcal{B}_{t,j,l}$, where \times here denotes the Cartesian product, and $\mathcal{B}_{r,i}$ and $\mathcal{B}_{t,j,l}$ are defined as

$$\mathcal{B}_{r,i} = \{u_r | \arg \min_{u_r} \|u_r - u_{r,i}\|^2\} \quad (6)$$

$$\mathcal{B}_{t,j,l} = \{(u_t, v_t) | \arg \min_{(u_t, v_t)} \|(u_t, v_t) - (u_{t,j}, v_{t,l})\|^2\} \quad (7)$$

where $u_{r,i}, u_{t,j}, v_{t,l}$ are sampled directional cosines, $i = 1, 2, \dots, N_k, j = 1, 2, \dots, N_x$ and $l = 1, 2, \dots, N_z$.

To guarantee the accuracy of this channel model, we select $N_k \geq M_k, N_x \geq M_x$ and $N_z \geq M_z$, and let $u_{r,i}, u_{t,j}$ and $v_{t,l}$ be uniformly sampled such that $\Delta_r u_{r,i}, \Delta_z u_{t,j}$ and $\Delta_x v_{t,l}$ are uniformly located in $[-0.5, 0.5]$. When N_k, N_x, N_z are large enough, the range of the directional cosines for each $\mathcal{B}_{r,i}$ and $\mathcal{B}_{t,j,l}$ will be very small, and the steering vectors $\mathbf{a}_r(u_r)$ and $\mathbf{a}_t(u_t, v_t)$ for

the points in each $\mathcal{B}_{r,i}$ and $\mathcal{B}_{t,j,l}$ can be well approximated by the steering vectors $\mathbf{a}_r(u_{r,i})$ and $\mathbf{a}_t(u_{t,j}, v_{t,l})$ at the sampling points $u_{r,i}$, $u_{t,j}$ and $v_{t,l}$. For brevity, we call the steering vectors at the sampling points the sampled steering vectors. With the sampled steering vectors, the channel \mathbf{H}_{km} can be approximated as

$$\mathbf{H}_{km} = \sum_{i,j,l} \sum_{u_r, u_t, v_t \in \mathcal{B}_d \cap (\mathcal{B}_{r,i} \times \mathcal{B}_{t,j,l})} g_k(u_r, u_t, v_t) \mathbf{a}_r(u_{r,i}) \mathbf{a}_t(u_{t,j}, v_{t,l})^H. \quad (8)$$

Let $\tilde{g}_k(u_{r,i}, u_{t,j}, v_{t,l})$ be defined as

$$\tilde{g}_k(u_{r,i}, u_{t,j}, v_{t,l}) = \sum_{u_r, u_t, v_t \in \mathcal{B}_d \cap (\mathcal{B}_{r,i} \times \mathcal{B}_{t,j,l})} g_k(u_r, u_t, v_t). \quad (9)$$

According to the definitions of the sampled steering vectors and the sets $\mathcal{B}_{r,i}$ and $\mathcal{B}_{t,j,l}$, the channel model in (8) can be rewritten as

$$\mathbf{H}_{km} = \sum_{i=1}^{N_k} \sum_{j=1}^{N_z} \sum_{l=1}^{N_x} \tilde{g}_k(u_{r,i}, u_{t,j}, v_{t,l}) \mathbf{a}_r(u_{r,i}) \mathbf{a}_t(u_{t,j}, v_{t,l})^H. \quad (10)$$

For this channel model, each sampled steering vector $\mathbf{a}_r(u_{r,i})$ at the user side represents a beam direction at the user side, and each sampled steering vector $\mathbf{a}_t(u_{t,j}, v_{t,l})$ at the BS side also represents a three dimensional (3D) beam direction at the BS side. Thus, we call this new channel model the beam domain channel model with sampled steering vectors, and the channel coefficients $\tilde{g}_k(u_{r,i}, u_{t,j}, v_{t,l})$ the beam domain channel coefficients. We assume the fading channels are wide-sense stationary uncorrelated scattering (WSSUS) Rayleigh fading. Then, it is reasonable to assume that the channel coefficients $\tilde{g}_k(u_{r,i}, u_{t,j}, v_{t,l})$ are independent complex Gaussian random variables with zero means and different variances.

In the following, we rewrite the channel model in (10) in a concrete matrix form. Let the matrix \mathbf{U} be defined by

$$\mathbf{U} = [\mathbf{a}_r(u_{r,1}), \mathbf{a}_r(u_{r,2}), \dots, \mathbf{a}_r(u_{r,N_k})]. \quad (11)$$

It denotes the $M_k \times N_k$ matrix of receive steering vectors. Let $N_t = N_z N_x$ and \mathbf{V} be the matrix of transmit steering vectors defined by $\mathbf{V}^H = \mathbf{V}_z^H \otimes \mathbf{V}_x^H \in \mathbb{C}^{N_t \times M_t}$, where

$$\mathbf{V}_z = [\mathbf{v}_z(u_{t,1}), \mathbf{v}_z(u_{t,2}), \dots, \mathbf{v}_z(u_{t,N_z})] \quad (12)$$

$$\mathbf{V}_x = [\mathbf{v}_x(v_{t,1}), \mathbf{v}_x(v_{t,2}), \dots, \mathbf{v}_x(v_{t,N_x})]. \quad (13)$$

Then, the channel model in (10) can be rewritten as

$$\mathbf{H}_{km} = \mathbf{U} \tilde{\mathbf{G}} \mathbf{V}^H \quad (14)$$

where $\tilde{\mathbf{G}}$ is called the beam domain channel matrix, and is defined by $(\mathbf{M}_k \odot \mathbf{W}_{km})$. The matrix \mathbf{M}_k is an $N_k \times N_t$ deterministic matrix with elements that denote the positive or negative square root of the variances of $\tilde{g}_k(u_{r,i}, u_{t,j}, v_{t,l})$, and \mathbf{W}_{km} is a complex Gaussian random matrix with independent and identically distributed (i.i.d.), zero mean and unit variance entries. Let $\mathbf{\Omega}_k$ denote the beam domain channel power matrices as

$$\mathbf{\Omega}_k = \mathbf{M}_k \odot \mathbf{M}_k. \quad (15)$$

For convenience, we call this analytical channel model the beam domain channel model in matrix form.

When $N_k = M_k$, $N_z = M_z$ and $N_x = M_x$, the matrix \mathbf{U} will become a DFT matrix and \mathbf{V} will be the Kronecker product of two DFT matrices, the proposed channel model reduces to the conventional beam domain channel model that straightforwardly extended from ULA [18], [28], [31] to UPA. However, the accuracy of the conventional beam domain channel model is not good enough when M_k , M_z , and M_x are of moderate sizes. When $N_k > M_k$ and $N_t > M_t$, \mathbf{U} and \mathbf{V}^H are not square matrices and thus can not be unitary matrices as in conventional beam domain MIMO channel for ULA. By sampling more directional cosines than those in the conventional beam domain channel model, the proposed new beam domain channel model with sampled steering vectors can model the statistical properties of the physical wireless channel more fine. For convenience, we define three fine factors as $F_k = \frac{N_k}{M_k}$, $F_z = \frac{N_z}{M_z}$ and $F_x = \frac{N_x}{M_x}$. In conclusion, with sampled steering vectors, the proposed new beam channel model generalizes the existing beam domain channel model for ULA to URA suitably and can have guaranteed accuracy.

C. Estimation of Beam Domain Channel Power Matrices and Instantaneous Channel Coefficients

In the new beam domain channel model (14), the matrix \mathbf{U} and \mathbf{V} are fixed matrices. Thus, the only statistical parameters need to be estimated is the beam domain channel power matrix $\mathbf{\Omega}_k$. To estimate the channel power matrices, we propose to use the received pilot signals. Let $\mathbf{X}_k \in \mathbb{C}^{M_k \times T}$ denote the uplink pilot signal transmitted by the k -th user. The received pilot signal $\mathbf{Y} \in \mathbb{C}^{M_t \times T}$ at the receive array of the BS can be written as

$$\mathbf{Y} = \sum_{k=1}^K \mathbf{H}_k^T \mathbf{X}_k + \mathbf{Z} = \sum_{k=1}^K \mathbf{V}^* \tilde{\mathbf{G}}_k^T \mathbf{U}^T \mathbf{X}_k + \mathbf{Z} \quad (16)$$

where $\tilde{\mathbf{G}}_k$ denotes the beam domain channel matrix as mentioned in the previous subsection, \mathbf{Z} is the noise matrix whose elements are independent and identically distributed (i.i.d.) complex Gaussian random variables with zero mean and variance σ_z^2 . Since the channel power matrices $\mathbf{\Omega}_k$ are statistical channel information, one sample of \mathbf{Y} at one slot is obviously not enough. Instead, we choose to use the samples of \mathbf{Y} from a certain number of time slots.

In the following, we propose a method to obtain the channel power matrices from the received pilot signals over a number of time slots. First, we notice that the beam domain channel matrix $\tilde{\mathbf{G}}_k$ has the following property provided in Theorem 1.

Theorem 1. *The beam domain channel matrix $\tilde{\mathbf{G}}_k$ satisfies*

$$\mathbb{E}\{(\mathbf{C}_1 \tilde{\mathbf{G}}_k \mathbf{C}_2^H) \odot (\mathbf{C}_1 \tilde{\mathbf{G}}_k \mathbf{C}_2^H)^*\} = \mathbf{T}_1 \mathbf{\Omega}_k \mathbf{T}_2 \quad (17)$$

where \mathbf{C}_1 and \mathbf{C}_2 are constant matrices, $\mathbf{T}_1 = \mathbf{C}_1 \odot \mathbf{C}_1^*$, and $\mathbf{T}_2 = \mathbf{C}_2^H \odot \mathbf{C}_2^T$.

Proof: The proof is provided in Appendix A. ■

For convenience, we obtain the transpose of \mathbf{Y} as

$$\mathbf{Y}^T = \sum_{k=1}^K \mathbf{X}_k^T \mathbf{H}_k + \mathbf{Z}^T = \sum_{k=1}^K \mathbf{X}_k^T \mathbf{U} \tilde{\mathbf{G}}_k \mathbf{V}^H + \mathbf{Z}^T. \quad (18)$$

For simplicity, we assume the pilot signals of different users are orthogonal, i.e., $\mathbf{X}_k \mathbf{X}_l^H = \mathbf{0}$, $k \neq l$. Under this assumption, we then obtain

$$\mathbf{U}^H \mathbf{X}_k^* \mathbf{Y}^T \mathbf{V} = \mathbf{U}^H \mathbf{X}_k^* \mathbf{X}_k^T \mathbf{U} \tilde{\mathbf{G}}_k \mathbf{V}^H \mathbf{V} + \mathbf{U}^H \mathbf{X}_k^* \mathbf{Z}^T \mathbf{V} \quad (19)$$

by left multiplying \mathbf{Y}^T with $\mathbf{U}^H \mathbf{X}_k^*$ and right multiplying it with \mathbf{V} . Let Φ_k denote

$$\mathbb{E}\{[(\mathbf{U}^H \mathbf{X}_k^* \mathbf{Y}^T \mathbf{V}) \odot (\mathbf{U}^H \mathbf{X}_k^* \mathbf{Y} \mathbf{V})^*]\}$$

we then obtain

$$\Phi_k = \mathbf{T}_{kr} \mathbf{\Omega}_k \mathbf{T}_t + \mathbf{O}_{kr} \mathbf{N} \mathbf{O}_t \quad (20)$$

where \mathbf{T}_{kr} , \mathbf{T}_t , \mathbf{O}_{kr} , \mathbf{N} and \mathbf{O}_t are defined as

$$\mathbf{T}_{kr} = (\mathbf{U}^H \mathbf{X}_k^* \mathbf{X}_k^T \mathbf{U}) \odot (\mathbf{U}^H \mathbf{X}_k^* \mathbf{X}_k^T \mathbf{U})^* \quad (21)$$

$$\mathbf{T}_t = \mathbf{V}^H \mathbf{V} \odot (\mathbf{V}^H \mathbf{V})^* \quad (22)$$

$$\mathbf{O}_{kr} = (\mathbf{U}^H \mathbf{X}_k^*) \odot (\mathbf{U}^H \mathbf{X}_k^*)^* \quad (23)$$

$$\mathbf{N} = \mathbb{E}\{\mathbf{Z}^T \odot (\mathbf{Z}^T)^*\} \quad (24)$$

$$\mathbf{O}_t = \mathbf{V} \odot \mathbf{V}^*. \quad (25)$$

When \mathbf{U} and \mathbf{V} are unitary matrices as in conventional beam domain channel models, the orthogonal pilot sequences for each user are also used, *i.e.*, $\mathbf{X}_k \mathbf{X}_k^H = \mathbf{I}$, and the noise are ignored, we have

$$\Phi_k = \Omega_k. \quad (26)$$

Thus, Ω_k is easy to obtain in conventional beam domain channel models. For the proposed new beam domain channel model, there are more works need to be done to obtain the channel power matrices Ω_k .

To estimate the channel power matrices Ω_k from Φ_k for general situation, we define an objective function first. Recall that the channel power matrices are defined as $\Omega_k = \mathbf{M}_k \odot \mathbf{M}_k$, we have that estimating \mathbf{M}_k is equivalent to estimating Ω_k . We define the function $f(\mathbf{M}_k)$ as the Kullback–Leibler (KL) divergence between Φ_k and $\mathbf{T}_{kr} \Omega_k \mathbf{T}_t + \mathbf{O}_{kr} \mathbf{N}_k \mathbf{O}_t$, *i.e.*, [32]

$$\begin{aligned} f(\mathbf{M}_k) = & \sum_{ij} [\Phi_k]_{ij} \log \frac{[\Phi_k]_{ij}}{[\mathbf{T}_{kr} \Omega_k \mathbf{T}_t + \mathbf{O}_{kr} \mathbf{N}_k \mathbf{O}_t]_{ij}} + \sum_{ij} [\mathbf{T}_{kr} \Omega_k \mathbf{T}_t + \mathbf{O}_{kr} \mathbf{N}_k \mathbf{O}_t]_{ij} \\ & - \sum_{ij} [\Phi_k]_{ij} \end{aligned} \quad (27)$$

Using the defined KL divergence function $f(\mathbf{M}_k)$, we are now able to formulate an optimization problem as

$$\mathbf{M}_k^* = \arg \min_{\mathbf{M}_k} f(\mathbf{M}_k) \quad (28)$$

which is an unconstrained optimization problem. Since there are items in $f(\mathbf{M}_k)$ that not related to \mathbf{M}_k , the above problem can be simplified to

$$\mathbf{M}_k^* = \arg \min_{\mathbf{M}_k} g(\mathbf{M}_k) \quad (29)$$

where $g(\mathbf{M}_k)$ is defined as

$$g(\mathbf{M}_k) = - \sum_{ij} [\Phi_k]_{ij} \log [\mathbf{T}_{kr} \Omega_k \mathbf{T}_t + \mathbf{O}_{kr} \mathbf{N}_k \mathbf{O}_t]_{ij} + \sum_{ij} [\mathbf{T}_{kr} \Omega_k \mathbf{T}_t]_{ij}. \quad (30)$$

To solve the optimization problem in (29), we compute the gradient of $g(\mathbf{M}_k)$ with respect to \mathbf{M}_k first. In the following theorem, we provide the gradients of the two items in the function $g(\mathbf{M}_k)$, respectively.

Theorem 2. *The gradients of the two items in $g(\mathbf{M}_k)$ can be obtained as*

$$\frac{\sum_{ij} [\mathbf{T}_{kr} (\mathbf{M}_k \odot \mathbf{M}_k) \mathbf{T}_t]_{ij}}{\partial \mathbf{M}_k} = (\mathbf{T}_t \mathbf{J} \mathbf{T}_{kr})^T \odot \mathbf{M}_k \quad (31)$$

and

$$\begin{aligned} & \frac{\partial \sum_{ij} [\Phi_k]_{ij} \log \mathbf{e}_i^H (\mathbf{T}_{kr} (\mathbf{M}_k \odot \mathbf{M}_k) \mathbf{T}_t + \mathbf{O}_{kr} \mathbf{N} \mathbf{O}_t) \mathbf{e}_j}{\partial \mathbf{M}_k} \\ &= (\mathbf{T}_t \mathbf{Q}^T \mathbf{T}_{kr})^T \odot \mathbf{M}_k \end{aligned} \quad (32)$$

where $[\mathbf{Q}]_{ij} = \frac{[\Phi_k]_{ij}}{[\mathbf{T}_{kr} (\mathbf{M}_k \odot \mathbf{M}_k) \mathbf{T}_t + \mathbf{O}_{kr} \mathbf{N} \mathbf{O}_t]_{ij}}$.

Proof: The proof is provided in Appendix B. ■

Using Theorem 2, we obtain the gradient of the function $g(\mathbf{M}_k)$ as

$$\frac{\partial g(\mathbf{M}_k)}{\partial \mathbf{M}_k} = (\mathbf{T}_t \mathbf{J} \mathbf{T}_{kr})^T \odot \mathbf{M}_k - (\mathbf{T}_t \mathbf{Q}^T \mathbf{T}_{kr})^T \odot \mathbf{M}_k. \quad (33)$$

By letting the gradient in the above equation equal zero, we obtain the first order optimal condition of the optimization problem (29) as

$$(\mathbf{T}_t \mathbf{J} \mathbf{T}_{kr})^T \odot \mathbf{M}_k = (\mathbf{T}_t \mathbf{Q}^T \mathbf{T}_{kr})^T \odot \mathbf{M}_k. \quad (34)$$

From the first order optimal condition, we then establish a fixed point equation as

$$[\mathbf{M}_k]_{ij} = \frac{[(\mathbf{T}_t \mathbf{Q}^T \mathbf{T}_{kr})^T + (\mathbf{T}_t \mathbf{J} \mathbf{T}_{kr})^T]_{ij}}{[2 * (\mathbf{T}_t \mathbf{J} \mathbf{T}_{kr})^T]_{ij}} [\mathbf{M}_k]_{ij}. \quad (35)$$

Using the fixed point equation provided in (35), we are now able to estimate \mathbf{M}_k from Φ_k . Although the convergence of (35) is hard to prove, it works pretty well in practice. Recall that Φ_k denotes the matrix $\mathbb{E}\{[(\mathbf{U}^H \mathbf{X}_k^* \mathbf{Y}^T \mathbf{V}) \odot (\mathbf{U}^H \mathbf{X}_k^* \mathbf{Y}^T \mathbf{V})^*]\}$. Thus, it is not possible to obtain the matrix Φ_k directly in practice. Instead, we use the sample averages of $(\mathbf{U}^H \mathbf{X}_k^* \mathbf{Y}^T \mathbf{V}) \odot (\mathbf{U}^H \mathbf{X}_k^* \mathbf{Y}^T \mathbf{V})^*$ over a number of time slots.

After obtaining the channel power matrices Ω_k , we can use it to obtain the instantaneous beam domain channel coefficients from the received pilot signals. For instantaneous beam domain channel coefficients, the received signal model can still be written as

$$\mathbf{Y}^T = \sum_{k=1}^K \mathbf{X}_k^T \mathbf{H}_k + \mathbf{Z}^T = \sum_{k=1}^K \mathbf{X}_k^T \mathbf{U} \tilde{\mathbf{G}}_k \mathbf{V}^H + \mathbf{Z}^T. \quad (36)$$

Vectorizing \mathbf{Y}^T , we obtain

$$\text{vec}(\mathbf{Y}^T) = \sum_{k=1}^K (\mathbf{V}^* \otimes \mathbf{X}_k^T \mathbf{U}) \text{vec}(\tilde{\mathbf{G}}_k) + \text{vec}(\mathbf{Z}^T). \quad (37)$$

By assuming the pilot signals of different users are orthogonal, we can obtain the MMSE estimate of $\text{vec}(\tilde{\mathbf{G}}_k)$ as

$$\text{vec}(\hat{\tilde{\mathbf{G}}}_k) = \mathbf{R}_{\tilde{\mathbf{g}}_k} (\mathbf{V}^* \otimes \mathbf{X}_k^T \mathbf{U})^H ((\mathbf{V}^* \otimes \mathbf{X}_k^T \mathbf{U}) \mathbf{R}_{\tilde{\mathbf{g}}_k} (\mathbf{V}^* \otimes \mathbf{X}_k^T \mathbf{U})^H + \sigma_z^2 \mathbf{I})^{-1} \text{vec}(\mathbf{Y}^T) \quad (38)$$

where $\mathbf{R}_{\tilde{\mathbf{g}}_k} = \text{diag}(\text{vec}(\Omega_k))$.

D. A Posteriori Beam Domain Channel Model

The channel model in (14) can be seen as an *a priori* model of the channels before channel estimation. Considering the impacts of channel aging, we can model the time variation of the beam domain channel from block to block by a first order Gauss-Markov process as

$$\tilde{\mathbf{G}}_{kmn} = \alpha_k(n-1)\tilde{\mathbf{G}}_{km1} + \sqrt{1 - \alpha_k(n-1)^2}(\mathbf{M}_k \odot \mathbf{W}_{kmn}) \quad (39)$$

where $\alpha_k(n)$ is the temporal correlation coefficient which is related to the moving speed.

The first order Gauss-Markov process in (39) can be used to obtain the *a posteriori* CSI of $\tilde{\mathbf{G}}_{kmn}$ after channel estimation being performed. Since the obtained channel estimation is that from the previous slot, we need to estimate $\tilde{\mathbf{G}}_{k(m-1)1}$. For simplicity, we assume the noise in the instantaneous beam domain channel estimation are very small in this paper, and thus the channel estimation error of $\text{vec}(\hat{\tilde{\mathbf{G}}}_{k(m-1)1})$ can be ignored. After the channel estimation, we obtain the *a posteriori* CSI of $\tilde{\mathbf{G}}_{kmn}$ as

$$\tilde{\mathbf{G}}_{kmn} = \alpha_k(N_b + n - 1)\tilde{\mathbf{G}}_{k(m-1)1} + \sqrt{1 - \alpha_k(N_b + n - 1)^2}(\mathbf{M}_k \odot \mathbf{W}_{kmn}) \quad (40)$$

where \mathbf{W}_{kmn} is a complex Gaussian random matrix with i.i.d., zero mean and unit variance entries.

In this paper, we are interested in the precoder design for massive MIMO downlink. To reduce the complexity, the precoder is carried once at each slot. Thus, we propose to obtain an approximate *a posteriori* CSI over each slot. The approximate *a posteriori* CSI at one slot is that obtained by using β_k to replace α_k , *i.e.*,

$$\tilde{\mathbf{G}}_{km} = \beta_k \tilde{\mathbf{G}}_{k(m-1)1} + \sqrt{1 - \beta_k^2}(\mathbf{M}_k \odot \mathbf{W}_{km}) \quad (41)$$

where β_k is given by

$$\beta_k = \left(\frac{|\alpha_k(N_b)|^2 + |\alpha_k(N_b + 1)|^2 + \dots + |\alpha_k(2N_b - 1)|^2}{N_b} \right)^{\frac{1}{2}}. \quad (42)$$

Finally, the *a posteriori* beam domain channel model can be written as

$$\mathbf{H}_{km} = \beta_k \mathbf{U} \tilde{\mathbf{G}}_{k(m-1)1} \mathbf{V}^H + \sqrt{1 - \beta_k^2} \mathbf{U}(\mathbf{M}_k \odot \mathbf{W}_{km}) \mathbf{V}^H. \quad (43)$$

With (43), the imperfect CSI for each user is modeled as an *a posteriori* beam domain channel model with both channel mean and channel variance information, which considers the impacts of practical antenna array and includes the effects of channel aging and spatial correlation. The model described in (43) can describe the imperfect CSI obtained by the BS in the practical

massive MIMO systems under various mobile scenarios. When β_k is very close to 1, it is equivalent to the quasi-static scenario. When β_k becomes very small, it can be used to describe high speed scenario. By setting the β_k according to their speeds, we are able to describe the channel uncertainties in various typical channel conditions in practical massive MIMO systems. Based on this channel model, we investigate the precoder design robust to the imperfect CSI at the BS in this work.

III. ROBUST LINEAR PRECODER DESIGN

In this section, we first present the problem formulation of the robust linear precoder design. We then provide iterative algorithms to solve the optimization problem.

A. Problem Formulation

We now consider the downlink transmission for slot m . For brevity, we omit the m in the subscript hereafter. Let \mathbf{x}_k denote the $M_k \times 1$ transmitted vector to the k -th UE at slot m . The covariance matrix of \mathbf{x}_k is the identity matrix \mathbf{I}_{d_k} . The received signal \mathbf{y}_k at the k -th UE for a single symbol interval at slot m can be written as

$$\mathbf{y}_k = \mathbf{H}_k \mathbf{P}_k \mathbf{x}_k + \mathbf{H}_k \sum_{l \neq k} \mathbf{P}_l \mathbf{x}_l + \mathbf{z}_k \quad (44)$$

where \mathbf{P}_k is the $M_t \times d_k$ precoding matrix of the k -th user, and \mathbf{z}_k is a complex Gaussian noise vector distributed as $\mathcal{CN}(0, \sigma_z^2 \mathbf{I}_{M_k})$.

Let $\bar{\mathbf{H}}_k$ denote $\beta_k \mathbf{H}_{k(m-1)1}$, the mean of \mathbf{H}_k , and $\check{\mathbf{H}}_k$ denote the random part of \mathbf{H}_k . The parameterized channel covariance matrix $\mathbb{E}\{\mathbf{H}_k \tilde{\mathbf{C}} \mathbf{H}_k^H\}$ can be obtained by

$$\mathbb{E}\{\mathbf{H}_k \tilde{\mathbf{C}} \mathbf{H}_k^H\} = \bar{\mathbf{H}}_k \tilde{\mathbf{C}} \bar{\mathbf{H}}_k^H + \mathbb{E}_{\check{\mathbf{H}}_k}\{\check{\mathbf{H}}_k \tilde{\mathbf{C}} \check{\mathbf{H}}_k^H\} \quad (45)$$

where $\tilde{\mathbf{C}} \in \mathbb{C}^{M_t \times M_t}$. For brevity, we define the matrix-valued function $\eta_k(\tilde{\mathbf{C}}) \in \mathbb{C}^{M_k \times M_k}$ as

$$\eta_k(\tilde{\mathbf{C}}) = \mathbb{E}_{\check{\mathbf{H}}_k}\{\check{\mathbf{H}}_k \tilde{\mathbf{C}} \check{\mathbf{H}}_k^H\}. \quad (46)$$

From the above equation and (43), we obtain

$$\eta_k(\tilde{\mathbf{C}}) = (1 - \beta_k^2) \mathbf{U} \mathbf{\Lambda}_k \mathbf{U}^H \quad (47)$$

where $\mathbf{\Lambda}_k$ is a diagonal matrix with its diagonal elements being computed from the channel power matrices $\mathbf{\Omega}_k$ as

$$[\mathbf{\Lambda}_k]_{ii} = \sum_{j=1}^{N_t} [\mathbf{\Omega}_k]_{ij} [\mathbf{V}^H \tilde{\mathbf{C}} \mathbf{V}]_{jj}. \quad (48)$$

Similarly, we can obtain the other parameterized channel covariance matrix $\mathbb{E}_{\mathbf{H}_k} \{\mathbf{H}_k^H \mathbf{C} \mathbf{H}_k\}$ and define the function $\tilde{\eta}_k(\mathbf{C}) \in \mathbb{C}^{M_t \times M_t}$, $\mathbf{C} \in \mathbb{C}^{M_k \times M_k}$ as

$$\begin{aligned} \tilde{\eta}_k(\mathbf{C}) &= \mathbb{E}_{\tilde{\mathbf{H}}_k} \{\tilde{\mathbf{H}}_k^H \mathbf{C} \tilde{\mathbf{H}}_k\} \\ &= (1 - \beta_k^2) \mathbf{V} \tilde{\mathbf{\Lambda}}_k \mathbf{V}^H \end{aligned} \quad (49)$$

where $\tilde{\mathbf{\Lambda}}_k$ is a diagonal matrix, and its diagonal elements are defined as

$$[\tilde{\mathbf{\Lambda}}_k]_{ii} = \sum_{j=1}^{N_k} [\mathbf{\Omega}_k]_{ji} [\mathbf{U}^H \mathbf{C} \mathbf{U}]_{jj}, \quad i = 1, 2, \dots, N_t. \quad (50)$$

We assume that the UEs obtain the perfect CSI of their corresponding channel matrices $\mathbf{H}_k \mathbf{P}_k$ from the precoding domain training signals. The DL training phase is included in the DL data transmission and omitted in the slot structure for simplicity. At each UE, we treat the aggregate interference-plus-noise $\mathbf{z}'_k = \mathbf{H}_k \sum_{l \neq k}^K \mathbf{P}_l \mathbf{x}_l + \mathbf{z}_k$ as Gaussian noise. Let \mathbf{R}_k denote the covariance matrix of \mathbf{z}'_k , we have that

$$\mathbf{R}_k = \sigma_z^2 \mathbf{I}_{M_k} + \sum_{l \neq k}^K \mathbb{E} \{ \mathbf{H}_k \mathbf{P}_l \mathbf{P}_l^H \mathbf{H}_k^H \}. \quad (51)$$

Using the function $\eta_k(\cdot)$, we can write explicitly the computation of \mathbf{R}_k as

$$\mathbf{R}_k = \sigma_z^2 \mathbf{I}_{M_k} + \sum_{l \neq k}^K \bar{\mathbf{H}}_k \mathbf{P}_l \mathbf{P}_l^H \bar{\mathbf{H}}_k^H + \sum_{l \neq k}^K \eta_k(\mathbf{P}_l \mathbf{P}_l^H). \quad (52)$$

We assume the covariance matrix \mathbf{R}_k is known at the k -th user. In such case, the expected rate of the k -th user at slot m is given by

$$\begin{aligned} \mathcal{R}_k &= \mathbb{E} \{ \log \det(\mathbf{R}_k + \mathbf{H}_k \mathbf{P}_k \mathbf{P}_k^H \mathbf{H}_k^H) \} - \mathbb{E} \{ \log \det(\mathbf{R}_k) \} \\ &= \mathbb{E} \{ \log \det(\mathbf{I}_{M_k} + \mathbf{R}_k^{-1} \mathbf{H}_k \mathbf{P}_k \mathbf{P}_k^H \mathbf{H}_k^H) \} \end{aligned} \quad (53)$$

where the expectation function $\mathbb{E}\{\cdot\}$ can be computed according to the *a posteriori* beam domain channel model provided in (43).

In this work, we are interested in finding the precoding matrices $\mathbf{P}_1, \mathbf{P}_2, \dots, \mathbf{P}_K$ that maximize the expected weighted sum-rate. The optimization problem can be formulated as

$$\begin{aligned} \mathbf{P}_1^\diamond, \mathbf{P}_2^\diamond, \dots, \mathbf{P}_K^\diamond &= \arg \max_{\mathbf{P}_1, \dots, \mathbf{P}_K} \sum_{k=1}^K w_k \mathcal{R}_k \\ \text{s.t.} \quad &\sum_{k=1}^K \text{tr}(\mathbf{P}_k \mathbf{P}_k^H) \leq 1, \end{aligned} \quad (54)$$

where w_k is the weight of the rate of the k -th user.

In the optimization problem (54), the inequality power constraint is used. In [13], it was mentioned that the inequality constraint for the WSR problem can be replaced by the equality constraint because the optimum is reached at the maximum transmit power. Thus, we use the equality power constraint in the following. With the equality power constraint, the optimization problem can be rewritten as

$$\begin{aligned} \mathbf{P}_1^\diamond, \mathbf{P}_2^\diamond, \dots, \mathbf{P}_K^\diamond = \arg \max_{\mathbf{P}_1, \dots, \mathbf{P}_K} & \sum_{k=1}^K w_k \mathcal{R}_k \\ \text{s.t.} & \sum_{k=1}^K \text{tr}(\mathbf{P}_k \mathbf{P}_k^H) = 1. \end{aligned} \quad (55)$$

B. Robust Precoder Design

In this subsection, we provide a robust precoder design for the optimization problem (55).

To obtain the structure of the optimal precoder, we start from deriving the gradient of the function f with respect to \mathbf{P}_k . From (53) and the derivative of $\log \det(\cdot)$ function [33], we obtain the gradient of \mathcal{R}_k with respect to \mathbf{P}_k as

$$\frac{\partial \mathcal{R}_k}{\partial \mathbf{P}_k^*} = \mathbf{E}_k \mathbf{P}_k \quad (56)$$

where \mathbf{E}_k is defined as

$$\mathbf{E}_k = w_k \mathbb{E} \{ \mathbf{H}_k^H \check{\mathbf{R}}_k^{-1} \mathbf{H}_k \} \quad (57)$$

and $\check{\mathbf{R}}_k = \mathbf{R}_k + \mathbf{H}_k \mathbf{P}_k \mathbf{P}_k^H \mathbf{H}_k^H$. Similarly, from (53) and the chain rule, we then obtain

$$\frac{\partial \mathcal{R}_l}{\partial \mathbf{P}_k^*} = -w_l \mathbf{F}_l \mathbf{P}_k \quad (58)$$

where \mathbf{F}_l is defined as

$$\mathbf{F}_l = \mathbb{E} \{ \mathbf{H}_l^H \mathbf{R}_l^{-1} \mathbf{H}_l \} - \mathbb{E} \{ \mathbf{H}_l^H \mathbb{E} \{ \check{\mathbf{R}}_l^{-1} \} \mathbf{H}_l \}. \quad (59)$$

Let the matrix \mathbf{B}_k be defined as

$$\mathbf{B}_k = \sum_{l \neq k}^K w_l \mathbf{F}_l. \quad (60)$$

The Euclidean gradient of the function f with respect to \mathbf{P}_k is then given by

$$\frac{\partial f}{\partial \mathbf{P}_k^*} = \mathbf{E}_k \mathbf{P}_k - \mathbf{B}_k \mathbf{P}_k. \quad (61)$$

The constraint in (55) can be seen as a manifold $\mathcal{M} = \{\mathbf{P}_1, \mathbf{P}_2, \dots, \mathbf{P}_k \mid \sum_{k=1}^K \text{tr}(\mathbf{P}_k \mathbf{P}_k^H) = 1\}$. If we convert the matrices $\mathbf{P}_1, \mathbf{P}_2, \dots, \mathbf{P}_k$ into a single vector as

$$\mathbf{p} = [\text{vec}(\mathbf{P}_1)^T \text{vec}(\mathbf{P}_2)^T \dots \text{vec}(\mathbf{P}_k)^T]^T \quad (62)$$

then this manifold \mathcal{M} becomes $\{\mathbf{p} \mid \mathbf{p}^H \mathbf{p} = 1\}$ and is actually a sphere manifold. The gradient of the function f with respect to \mathbf{p} on the sphere \mathcal{M} is given by projecting the Euclidean gradient $\frac{\partial f}{\partial \mathbf{p}}$ onto the tangent space $T_s \mathcal{M}$ of the manifold \mathcal{M} at \mathbf{p} , *i.e.* [34],

$$\text{grad}_{\mathbf{p}} f = (\mathbf{I} - \mathbf{p} \mathbf{p}^H) \frac{\partial f}{\partial \mathbf{p}^*}. \quad (63)$$

From the definition of the vector \mathbf{p} , its Euclidean gradient of the function f can be obtained from the Euclidean gradient of the function f with respect to \mathbf{P}_k .

From the definition of the Riemannian gradient on the sphere, we have that

$$\text{grad}_{\mathbf{p}} f = \frac{\partial f}{\partial \mathbf{p}^*} - \mu \mathbf{p} \quad (64)$$

where μ is given by $\mathbf{p}^H \frac{\partial f}{\partial \mathbf{p}^*}$. For convenience, we rewritten the Riemannian gradient with respect to \mathbf{p} to the Riemannian gradient with respect to \mathbf{P}_k as

$$\begin{aligned} \text{grad}_{\mathbf{P}_k} f &= \frac{\partial f}{\partial \mathbf{P}_k^*} - \mu \mathbf{P}_k \\ &= \mathbf{E}_k \mathbf{P}_k - \mathbf{B}_k \mathbf{P}_k - \mu \mathbf{P}_k, \quad k = 1, 2, \dots, K \end{aligned} \quad (65)$$

where μ is given by

$$\mu = \sum_{k=1}^K \text{tr}((\mathbf{P}_k^H (\mathbf{E}_k - \mathbf{B}_k) \mathbf{P}_k)). \quad (66)$$

By viewing the constraint as a manifold, the constrained optimization problem in (55) becomes an unconstrained optimization problem on the manifold \mathcal{M} as

$$\mathbf{P}_1^\diamond, \mathbf{P}_2^\diamond, \dots, \mathbf{P}_K^\diamond = \arg \max_{\mathbf{P}_1, \dots, \mathbf{P}_K \in \mathcal{M}} \sum_{k=1}^K w_k \mathcal{R}_k. \quad (67)$$

Then, we obtain the following theorem.

Theorem 3. *The stationary points for the optimization problem (55) satisfy*

$$\mathbf{E}_k \mathbf{P}_k - \mathbf{B}_k \mathbf{P}_k - \mu \mathbf{P}_k = \mathbf{0}, \quad k = 1, 2, \dots, K \quad (68)$$

Proof: The result is obtained by setting the Riemannian gradient of the function f on the manifold \mathcal{M} to zero. ■

In [27], a precoder design that converges to a stationary point is derived by using the minorize-maximize (MM) algorithm. We can also use the MM algorithm here to obtain a precoder design that converges to a stationary point of the optimization problem (55). However, the derive process of the MM algorithm is a bit complicated. Thus, we obtain an iterative precoder design which has a similar structure to that in [27] directly from the conditions provided in Theorem 3.

To obtain an iterative precoder design similar to that in [27], we first define the matrix \mathbf{B} as

$$\mathbf{B} = \sum_{k=1}^K w_k \mathbf{F}_k \quad (69)$$

and the matrix \mathbf{A}_k as

$$\mathbf{A}_k = w_k \mathbf{F}_k + w_k \mathbf{E}_k = w_k \mathbb{E}\{\mathbf{H}_k^H \mathbf{R}_k^{-1} \mathbf{H}_k\} - \mathbb{E}\{\mathbf{H}_l^H (\mathbb{E}\{\check{\mathbf{R}}_l^{-1}\} - \check{\mathbf{R}}_l^{-1}) \mathbf{H}_l\}. \quad (70)$$

Then, the condition in Theorem 3 becomes

$$\mathbf{A}_k \mathbf{P}_k - \mathbf{B} \mathbf{P}_k - \mu \mathbf{P}_k = \mathbf{0}, \quad k = 1, 2, \dots, K \quad (71)$$

where μ becomes

$$\mu = \sum_{k=1}^K \text{tr}((\mathbf{P}_k^H (\mathbf{A}_k - \mathbf{B}) \mathbf{P}_k). \quad (72)$$

Thus, we obtain a similar iterative process to that in [27] as

$$\mathbf{P}_k = (\mathbf{B} + \mu \mathbf{I})^{-1} \mathbf{A}_k \mathbf{P}_k \quad (73)$$

where \mathbf{B} and \mathbf{A}_k are related to the iterative process. By using (73), we obtain a robust precoder design for 3D massive MIMO with imperfect CSI.

We now summarize the algorithm for the design of robust linear precoder for massive MIMO with UPA and imperfect CSI.

Algorithm 1: Robust linear precoder design

Step 1: Set $d = 0$. Randomly generate $\mathbf{P}_1[d], \mathbf{P}_2[d], \dots, \mathbf{P}_K[d]$ and normalize them to satisfy the power constraint.

Step 2: Calculate $\mathbf{R}_k[d]$ according to

$$\mathbf{R}_k[d] = \sigma_z^2 \mathbf{I}_{M_k} + \sum_{l \neq k} \bar{\mathbf{H}}_k \mathbf{P}_l[d] (\mathbf{P}_l[d])^H \bar{\mathbf{H}}_k^H + \sum_{l \neq k} \eta_k (\mathbf{P}_l[d] (\mathbf{P}_l[d])^H)$$

where the computation of $\eta_k(\cdot)$ is provided in (47).

Step 3: Compute $\mathbf{A}_k[d]$ and $\mathbf{B}[d]$ according to

$$\begin{aligned}\mathbf{A}_k[d] &= \mathbb{E}\{\mathbf{H}_k^H(\mathbf{R}_k[d])^{-1}\mathbf{H}_k\} - \mathbb{E}\{\mathbf{H}_k^H(\mathbb{E}\{\check{\mathbf{R}}_k[d]^{-1}\} - (\check{\mathbf{R}}_k[d])^{-1})\mathbf{H}_k\} \\ \mathbf{B}[d] &= \sum_{k=1}^K (\mathbb{E}\{\mathbf{H}_k^H(\mathbf{R}_k[d])^{-1}\mathbf{H}_k\} - \mathbb{E}\{\mathbf{H}_k^H\mathbb{E}\{\check{\mathbf{R}}_k[d]^{-1}\}\mathbf{H}_k\}).\end{aligned}$$

Step 4: Compute μ by

$$\mu = \sum_{k=1}^K \text{trace}((\mathbf{P}_k[d])^H(\mathbf{A}_k[d] - \mathbf{B}[d])\mathbf{P}_k[d]).$$

Step 5: Update $\mathbf{P}_k[d+1]$ by

$$\mathbf{P}_k[d+1] = (\mathbf{B}[d] + \mu\mathbf{I})^{-1}\mathbf{A}_k[d]\mathbf{P}_k[d].$$

Normalize the precoders to satisfy the power constraint. Set $d = d + 1$.

Repeat Step 2 through Step 5 until convergence or until a pre-set target is reached.

However, the problem is still not solved since Step 3 are hard to compute because there is no explicit formula to compute the expected function. The deterministic equivalent approach [35] is a successful method to derive the approximate capacity for various MIMO channels. It has been widely investigated in literature [36]–[39] based on random matrix theory and operator-valued free probability [40]. By replacing the expected rates of all users in (55) with their deterministic equivalents, a similar precoder design to that in (73) with the counterparts of (57) and (59) being easy to compute can be obtained. Furthermore, we can obtain an algorithm that similar to Algorithm 1 with Step 3 being replaced by the counterparts based on the deterministic equivalent method.

Although the problem (55) can be solved by using the deterministic equivalent method, its complexity might not be satisfactory in practice. In the next subsection, we provide a low complexity robust linear precoder design of the problem (55) by replacing the expected rates of all users with their approximations.

C. Low Complexity Robust Linear Precoder Design

The complexity of the robust precoder design in the previous section is too high because the expected rate of each user is involved in the optimization problem. To provide a simpler low complexity robust linear precoder design, we can choose a simpler objective function. Since the

$\log \det(\cdot)$ is a convex function, we can obtain an upper bound of the expected rate of each user as

$$\mathcal{R}_k^{ub} = \log \det(\mathbf{I}_{M_k} + \mathbf{R}_k^{-1} \mathbb{E}\{\mathbf{H}_k \mathbf{P}_k \mathbf{P}_k^H \mathbf{H}_k^H\}). \quad (74)$$

Compared with the expected rate, the upper bound is easy to compute. Using the upper bound, we formulate a new optimization problem as

$$\begin{aligned} \mathbf{P}_1^\diamond, \mathbf{P}_2^\diamond, \dots, \mathbf{P}_K^\diamond = \arg \max_{\mathbf{P}_1, \dots, \mathbf{P}_K} & \sum_{k=1}^K w_k \mathcal{R}_k^{ub} \\ \text{s.t.} & \sum_{k=1}^K \text{tr}(\mathbf{P}_k \mathbf{P}_k^H) = 1. \end{aligned} \quad (75)$$

By using the upper bounds of the expected rates, the gradient of \mathcal{R}_k^{ub} with respect to \mathbf{P}_k becomes

$$\frac{\partial \mathcal{R}_k^{ub}}{\partial \mathbf{P}_k^*} = \mathbf{E}'_k \mathbf{P}_k \quad (76)$$

where \mathbf{E}'_k is defined as

$$\mathbf{E}'_k = w_k \mathbb{E}\{\mathbf{H}_k^H (\check{\mathbf{R}}'_k)^{-1} \mathbf{H}_k\}. \quad (77)$$

with $\check{\mathbf{R}}'_k = \mathbb{E}\{\check{\mathbf{R}}_k\}$. Similarly, the gradient of \mathcal{R}_l^{ub} with respect to \mathbf{P}_k becomes

$$\frac{\partial \mathcal{R}_l^{ub}}{\partial \mathbf{P}_k^*} = -w_l \mathbf{F}'_l \mathbf{P}_k \quad (78)$$

where \mathbf{F}'_l is defined as

$$\mathbf{F}'_l = \mathbb{E}\{\mathbf{H}_l^H \mathbf{R}_l^{-1} \mathbf{H}_l\} - \mathbb{E}\{\mathbf{H}_l^H (\check{\mathbf{R}}'_l)^{-1} \mathbf{H}_l\}. \quad (79)$$

Let the matrix \mathbf{B}'_k be defined as

$$\mathbf{B}'_k = \sum_{l \neq k}^K w_l \mathbf{F}'_l. \quad (80)$$

Then, the gradient of the function f with respect to \mathbf{P}_k is then given by

$$\frac{\partial f}{\partial \mathbf{P}_k^*} = \mathbf{E}'_k \mathbf{P}_k - \mathbf{B}'_k \mathbf{P}_k. \quad (81)$$

Compared with that in (61), the gradient in (81) is now easy to compute. Thus, we can compute this gradient directly. Similarly as presented in the previous subsection, to obtain an iterative precoder design, we let the matrices \mathbf{B}' and \mathbf{A}'_k be defined as

$$\mathbf{B}' = \sum_{k=1}^K w_k \mathbf{F}'_k \quad (82)$$

$$\mathbf{A}'_k = w_k \mathbb{E}\{\mathbf{H}_k^H \mathbf{R}_k^{-1} \mathbf{H}_k\}. \quad (83)$$

The stationary points now satisfy

$$\mathbf{A}'_k \mathbf{P}_k - \mathbf{B}' \mathbf{P}_k - \mu' \mathbf{P}_k = \mathbf{0}, \quad k = 1, 2, \dots, K \quad (84)$$

where

$$\mu' = \sum_{k=1}^K \text{tr}((\mathbf{P}_k^H (\mathbf{A}'_k - \mathbf{B}') \mathbf{P}_k)). \quad (85)$$

Finally, the low complexity precoder can be obtained iteratively as

$$\mathbf{P}_k = (\mathbf{B}' + \mu \mathbf{I})^{-1} \mathbf{A}'_k \mathbf{P}_k. \quad (86)$$

When the CSI is perfectly known at the BS, the upper bound of the expected rate used in this subsection will become the exact rate. In such case, the iterative formula of the precoder obtained in (86) becomes

$$\mathbf{P}_k = \left(\sum_{k=1}^K w_k \mathbf{H}_k^H (\mathbf{R}_k^{-1} - \check{\mathbf{R}}_k^{-1}) \mathbf{H}_k + \mu \mathbf{I} \right)^{-1} (w_k \mathbf{H}_k^H \mathbf{R}_k^{-1} \mathbf{H}_k) \mathbf{P}_k \quad (87)$$

which is equivalent to the iterative WMMSE precoder. Observing (87), we find $w_k \mathbf{H}_k^H \mathbf{R}_k^{-1} \mathbf{H}_k$ includes the information about the spatial directions that can be used to transmit the signal for the k -th user, whereas $\sum_{k=1}^K w_k \mathbf{H}_k^H (\mathbf{R}_k^{-1} - \check{\mathbf{R}}_k^{-1}) \mathbf{H}_k + \mu \mathbf{I}$ includes the information about the spatial directions that will cause interference. At each iteration, the precoder \mathbf{P}_k is first enhanced by $w_k \mathbf{H}_k^H \mathbf{R}_k^{-1} \mathbf{H}_k$ and then filtered by $\left(\sum_{k=1}^K w_k \mathbf{H}_k^H (\mathbf{R}_k^{-1} - \check{\mathbf{R}}_k^{-1}) \mathbf{H}_k + \mu \mathbf{I} \right)^{-1}$. Thus, the resulted precoders can guarantee the gains of the signal and keep the interference small at the same time.

Furthermore, when \mathbf{H}_k has zero mean values, \mathbf{A}'_k becomes the weighted channel covariance matrix of the k -th user, and $\mathbf{B}' + \mu \mathbf{I}$ is dominated by the weighted channel covariance matrices of the interference users. Using (86), we can still obtain the precoders that guarantee the gains of the signal and keep the interference small at the same time. For general cases where \mathbf{H}_k has nonzero mean values, the situations are similar and the obtained precoder can thus still achieve good performance. When N_t becomes large, the complexity of the matrix inversion in (86) might be too high. To further reduce the computational complexity, the truncated conjugate gradient (CG) method can be used to solve (86).

We now summarize the algorithm for the design of the low complexity robust linear precoder for massive MIMO with UPA and imperfect CSI.

Algorithm 2: Low complexity robust linear precoder design

Step 1: Set $d = 0$. Randomly generate $\mathbf{P}_1[d], \mathbf{P}_2[d], \dots, \mathbf{P}_K[d]$ and normalize them to satisfy the power constraint.

Step 2: Calculate $\mathbf{R}_k[d]$ according to

$$\begin{aligned}\mathbf{R}_k[d] &= \sigma_z^2 \mathbf{I}_{M_k} + \sum_{l \neq k}^K \bar{\mathbf{H}}_k \mathbf{P}_l[d] (\mathbf{P}_l[d])^H \bar{\mathbf{H}}_k^H + \sum_{l \neq k}^K \eta_k (\mathbf{P}_l[d] (\mathbf{P}_l[d])^H) \\ \check{\mathbf{R}}'_k[d] &= \mathbf{R}_k[d] + \bar{\mathbf{H}}_k \mathbf{P}_k[d] (\mathbf{P}_k[d])^H \bar{\mathbf{H}}_k^H + \eta_k (\mathbf{P}_k[d] (\mathbf{P}_k[d])^H)\end{aligned}$$

where the computation of $\eta_k(\cdot)$ is provided in (47).

Step 3: Compute $\mathbf{A}'_k[d]$ and $\mathbf{B}'[d]$ according to

$$\begin{aligned}\mathbf{A}'_k[d] &= \bar{\mathbf{H}}_k^H (\mathbf{R}_k[d])^{-1} \bar{\mathbf{H}}_k + \tilde{\eta}_k ((\mathbf{R}_k[d])^{-1}) \\ \mathbf{B}'[d] &= \sum_{k=1}^K \left(\bar{\mathbf{H}}_k^H ((\mathbf{R}_k[d])^{-1} - (\check{\mathbf{R}}'_k[d])^{-1}) \bar{\mathbf{H}}_k + \tilde{\eta}_k ((\mathbf{R}_k[d])^{-1} - (\check{\mathbf{R}}'_k[d])^{-1}) \right)\end{aligned}$$

where the computation of $\tilde{\eta}_k(\cdot)$ is provided in (49).

Step 4: Compute μ by

$$\mu = \sum_{k=1}^K \text{trace}((\mathbf{P}_k[d])^H (\mathbf{A}'_k[d] - \mathbf{B}'[d]) \mathbf{P}_k[d]).$$

Step 5: Update $\mathbf{P}_k[d+1]$ by

$$\mathbf{P}_k[d+1] = (\mathbf{B}'[d] + \mu \mathbf{I})^{-1} \mathbf{A}'_k[d] \mathbf{P}_k[d].$$

Normalize the precoders to satisfy the power constraint. Set $d = d + 1$.

Repeat Step 2 through Step 5 until convergence or until a pre-set target is reached.

IV. SIMULATION RESULTS

In this section, we provide simulation results to show the performance of the proposed precoder. We use the widely used QuaDRiGa channel model [41]. For simplicity, the path loss model and shadow fading are disabled. We set the center frequency to 4.8 GHz. The simulation scenario is set to “3GPP_38.901_UMa_NLOS”. The total transmit power is set as $P = 1$. The type of the antenna array used at the BS is “3gpp-3d” with $D_{in} = 1$. We consider a massive MIMO with $M_t = 128$ antennas at the BS, where $M_x = 16$ and $M_z = 8$. The number of users is set as $K = 40$, and each user is equipped with single antenna. We only use the setting $N_t \geq M_t$ in the BS side and set $F_k = 1$ for simplicity. The layout of this massive MIMO system is plotted in Fig. 3, where the location of the BS is at $(0, 0, 25)$, and the users are randomly generated

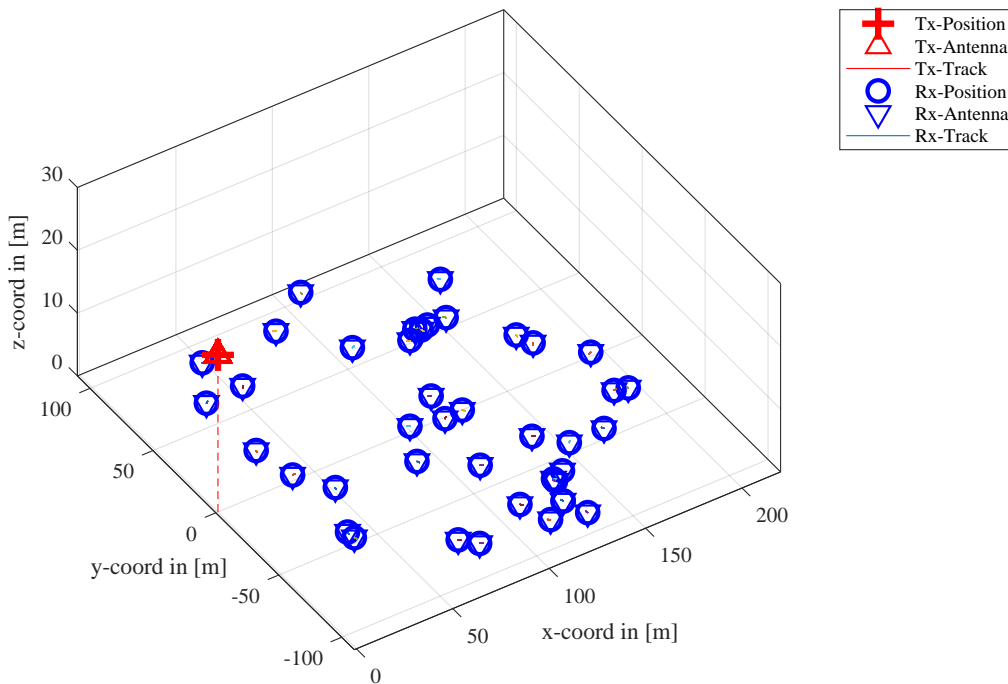


Fig. 3. The layout of a massive MIMO with $M_t = 128$, $M_k = 1$, $K = 40$.

in a circle with radius $r = 100\text{m}$ around $(0, 0, 0)$ at 1.5m height and then move 100m to the right side of the BS. For simplicity, the SNR is set as $\text{SNR} = \frac{1}{\sigma_z^2}$. The lengths of all the simulated tracks are set to be the same 2 m .

After generating the channels using QuaDRiGa, we use equation (35) to obtain the channel power matrices Ω_k . Furthermore, we compute the empirical temporal correlation coefficients $\alpha_k(n)$ and β_k from the sample of channel matrices. With the channel power matrices Ω_k and the temporal correlation coefficient β_k , we are able to perform Algorithms 1 and 2. Fig. 4 plots the sum-rate performance of Algorithms 1 and 2, the RZF precoder and the SLNR precoder for the considered massive MIMO downlink. The length of one slot is set to 0.5 ms . For Algorithm 1, the deterministic equivalent method is used to compute the expectations in Step 3. To show the impact of channel aging, the speed of the users are set to 30 , 120 and 250 km/h . The fine factors of sampled directional cosines are set as $F_x = F_z = 2$. The number of iterations is 20 . We use the RZF precoders as the initial values of Algorithms 1 and 2. From Fig. 4, we observe that the performance of Algorithms 1 and 2 are almost the same, and Algorithm 2 outperforms the RZF

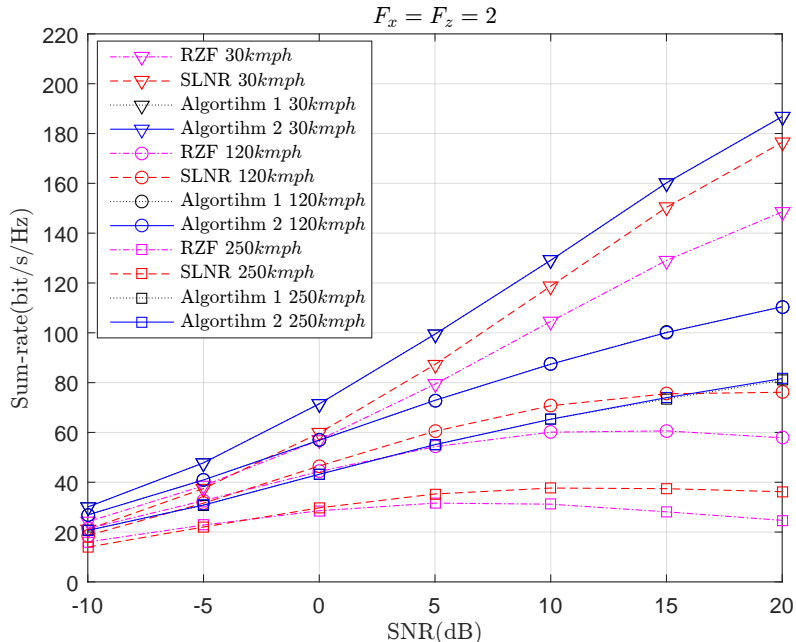


Fig. 4. The sum-rate performance of the four types of precoder for a massive MIMO downlink with $M_t = 128$, $M_k = 1$, $K = 40$ and $F_x = F_z = 2$.

precoder and the SLNR precoder significantly at all three cases. The sum-rate of Algorithm 2 is about 1.25 times of that of the RZF precoder at SNR=20dB for the 30kmph case. It increases to 1.98 and 3.26 times of that of the RZF precoder for the latter two cases. Meanwhile, the sum-rate of Algorithm 2 is about 1.06, 1.48 and 2.28 times of that of the SLNR precoder for the 30, 120 and 250 km/h cases. The results show that the performance gain of robust linear precoders are more significant in high speed scenario.

In the previous simulations, we have set the fine factors of steering vectors at the BS side as $F_x = F_z = 2$. To investigate the impacts of the fine factors F_x and F_z , we simulate the sum-rate of Algorithm 2 for three cases: case one where $F_x = F_z = 4$, case two where $F_x = F_z = 2$ and case three where $F_x = F_z = 1$. The case $F_x = F_z = 1$ is equivalent to using the conventional DFT based beam domain channel model. The length of one slot is still set to 0.5 ms. We consider both the moderate and high speed scenario. The users' speed is set to 120km/h and 250km/h. The simulation results of the sum-rates are shown in Fig. 5. From the results, we observe that using large F_x and F_z achieves better performance. The sum-rate of the $F_x = F_z = 2$ case is about 1.18 times of the case with $F_x = F_z = 1$ at SNR=30dB for the moderate speed scenario.

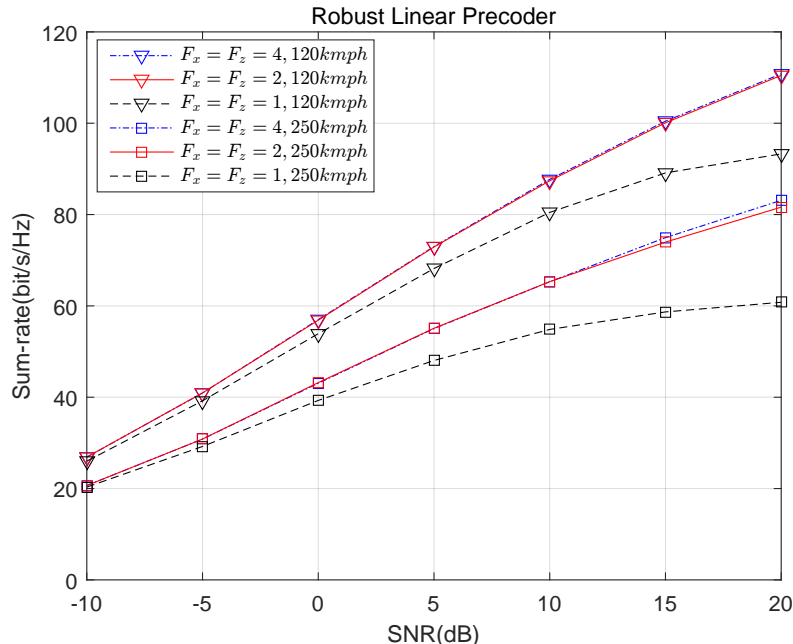


Fig. 5. The sum-rate performance of the low complexity robust linear precoders with different fine factors for a massive MIMO downlink with $M_t = 128$, $M_k = 1$, $K = 40$.

It increases to 1.30 times of that of the latter one for the high speed scenario. The results show that using the conventional beam domain channel model based on the DFT matrices is not good enough for moderate number of antennas in each row and column of the antenna array. Thus, the robust precoder designed by using the new beam domain channel model based on the matrix of sampled steering vectors is superior to that by the conventional beam domain channel model for the considered massive MIMO with UPA. Furthermore, the performance gain of the case $F_x = F_z = 4$ is negligible compared to that of $F_x = F_z = 2$. Thus, to achieve a good precoding performance, we do not need to increase the fine factors F_x and F_z too much.

We then study the convergence behavior of the proposed precoder. For simplicity, the speed of the users is set to 250 km/h. We still use the RZF precoders as the initial values of the robust precoders. The number of the iterations is 20. Fig. 6 plots the sum-rates of the proposed precoder at each iteration for three different SNRs. From Fig. 6, we see that the proposed algorithm for all three cases quickly converges. We also observe that it takes more iterations to converge as the SNR increases. At SNR= 0dB, only 10 iterations are needed for the convergence, whereas 20 iterations are needed at SNR= 20dB. The number of iterations can be further reduced if we

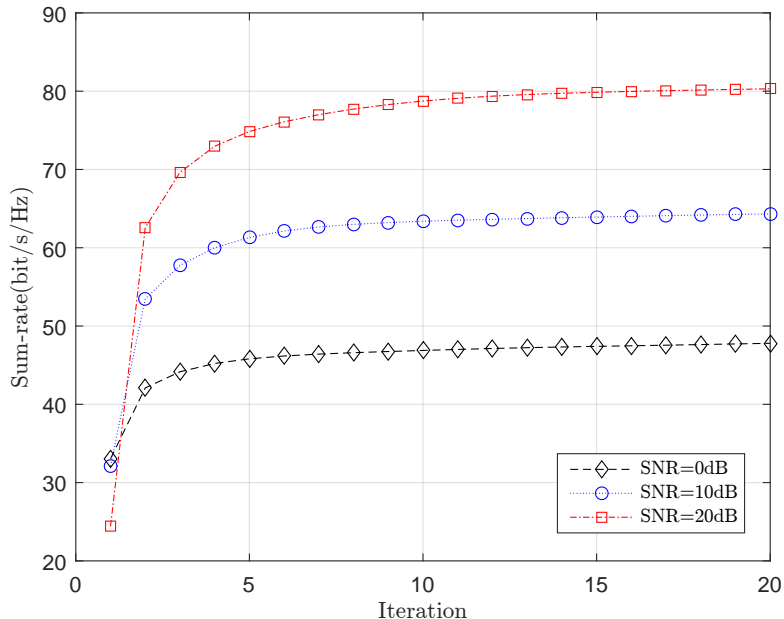


Fig. 6. The sum-rate performance of the robust linear precoder at each iteration for three different SNRs.

use better initial values such as the precoder from previous slot.

V. CONCLUSION

In this paper, we investigated the robust linear precoder design for massive MIMO downlink with UPA and imperfect CSI, which was represented by an *a posteriori* beam domain channel model. The *a posteriori* beam domain channel model is established based on a new *a priori* beam domain channel model. In the new beam domain channel model, we used the matrix of sampled steering vectors to represent the virtual spatial directions in the channel model. With the sampled steering vectors, the new beam domain channel model generalizes the existing beam domain channel model for ULA to URA with guaranteed accuracy. We also presented a novel method to obtain the channel power matrices and instantaneous beam domain channel coefficients from the received pilot signals. On the basis of the *a posteriori* beam domain channel model, the considered optimization problem of robust precoder design was maximizing the expected weighted sum-rate under a total power constraint. We transformed the constrained optimization problem into an unconstrained optimization problem on a Riemannian manifold. Under the framework of the manifold optimization, we derived an iterative algorithm to obtain the optimal

precoders. Furthermore, we proposed a low complexity robust precoder design by replacing the expected rates in the objective function with their upper bounds. Simulation results showed that the proposed precoders can achieve significantly performance gain compared to the RZF precoder and the SLNR precoder.

APPENDIX A
PROOF OF THEOREM 1

First, from the property of Hadmard product, we have

$$\begin{aligned}
& [\mathbb{E}\{(\mathbf{C}_1 \tilde{\mathbf{G}}_k \mathbf{C}_2^H) \odot (\mathbf{C}_1 \tilde{\mathbf{G}}_k \mathbf{C}_2^H)^*\}]_{ij} \\
&= \mathbb{E}\{[\mathbf{C}_1 \tilde{\mathbf{G}}_k \mathbf{C}_2^H]_{ij} [\mathbf{C}_1 \tilde{\mathbf{G}}_k \mathbf{C}_2^H]^*_{ij}\} \\
&= \mathbb{E}\left\{\sum_{s_1=1}^{N_k} \sum_{s_2=1}^{N_t} [\mathbf{C}_1]_{is_1} [\tilde{\mathbf{G}}_k]_{s_1 s_2} [\mathbf{C}_2^H]_{s_2 j} \sum_{t_1=1}^{N_k} \sum_{t_2=1}^{N_t} [\mathbf{C}_1]^*_{it_1} [\tilde{\mathbf{G}}_k]^*_{t_1 t_2} [\mathbf{C}_2^H]^*_{t_2 j}\right\}. \tag{88}
\end{aligned}$$

Then, it follows that

$$\begin{aligned}
& [\mathbb{E}\{(\mathbf{C}_1 \tilde{\mathbf{G}}_k \mathbf{C}_2^H) \odot (\mathbf{C}_1 \tilde{\mathbf{G}}_k \mathbf{C}_2^H)^*\}]_{ij} \\
&= \mathbb{E}\left\{\sum_{s_1=1}^{N_k} \sum_{s_2=1}^{N_t} \sum_{t_1=1}^{N_k} \sum_{t_2=1}^{N_t} [\mathbf{C}_1]_{is_1} [\tilde{\mathbf{G}}_k]_{s_1 s_2} [\mathbf{C}_2^H]_{s_2 j} [\mathbf{C}_1]^*_{it_1} [\tilde{\mathbf{G}}_k]^*_{t_1 t_2} [\mathbf{C}_2^H]^*_{t_2 j}\right\} \\
&= \sum_{s_1=1}^{N_k} \sum_{s_2=1}^{N_t} \sum_{t_1=1}^{N_k} \sum_{t_2=1}^{N_t} [\mathbf{C}_1]_{is_1} [\mathbf{C}_2^H]_{s_2 j} [\mathbf{C}_1]^*_{it_1} [\mathbf{C}_2^H]^*_{t_2 j} \mathbb{E}\{[\tilde{\mathbf{G}}_k]_{s_1 s_2} [\tilde{\mathbf{G}}_k]^*_{t_1 t_2}\}. \tag{89}
\end{aligned}$$

From $\mathbb{E}\{[\tilde{\mathbf{G}}_k]_{s_1 s_2} [\tilde{\mathbf{G}}_k]^*_{t_1 t_2}\} = [\mathbf{\Omega}_k]_{s_1 s_2} \delta(s_1 - t_1) \delta(s_2 - t_2)$, we then obtain

$$\begin{aligned}
& [\mathbb{E}\{(\mathbf{C}_1 \tilde{\mathbf{G}}_k \mathbf{C}_2^H) \odot (\mathbf{C}_1 \tilde{\mathbf{G}}_k \mathbf{C}_2^H)^*\}]_{ij} \\
&= \sum_{s_1=1}^{N_k} \sum_{s_2=1}^{N_t} [\mathbf{C}_1]_{is_1} [\mathbf{C}_2^H]_{s_2 j} [\mathbf{C}_1]^*_{is_1} [\mathbf{C}_2^H]^*_{s_2 j} [\mathbf{\Omega}_k]_{s_1 s_2} \\
&= \sum_{s_1=1}^{N_k} \sum_{s_2=1}^{N_t} [\mathbf{C}_1 \odot \mathbf{C}_1^*]_{is_1} [\mathbf{\Omega}_k]_{s_1 s_2} [\mathbf{C}_2^H \odot \mathbf{C}_2^T]_{s_2 j}. \tag{90}
\end{aligned}$$

Let $\mathbf{T}_1 = \mathbf{C}_1 \odot \mathbf{C}_1^*$ and $\mathbf{T}_2 = \mathbf{C}_2^H \odot \mathbf{C}_2^T$, we finally obtain

$$[\mathbb{E}\{(\mathbf{C}_1 \tilde{\mathbf{G}}_k \mathbf{C}_2^H) \odot (\mathbf{C}_1 \tilde{\mathbf{G}}_k \mathbf{C}_2^H)^*\}]_{ij} = [\mathbf{T}_1 \mathbf{\Omega}_k \mathbf{T}_2]_{ij}. \tag{91}$$

APPENDIX B
PROOF OF THEOREM 2

We have

$$\begin{aligned}
& \sum_{ij} [\mathbf{T}_{kr}(\mathbf{M}_k \odot \mathbf{M}_k)\mathbf{T}_t]_{ij} \\
&= \partial \sum_{ij} \mathbf{e}_i^H \mathbf{T}_{kr}(\mathbf{M}_k \odot \mathbf{M}_k)\mathbf{T}_t \mathbf{e}_j \\
&= \sum_{uv} \sum_{ij} \mathbf{e}_i^H \mathbf{T}_{kr} \mathbf{e}_u \mathbf{e}_v^H \mathbf{T}_t \mathbf{e}_j [\mathbf{M}_k]_{uv} \\
&= \sum_{uv} \left[\sum_{ij} \mathbf{T}_t \mathbf{e}_j \mathbf{e}_i^H \mathbf{T}_{kr} \right]_{vu} [\mathbf{M}_k]_{uv} [\mathbf{M}_k]_{uv} \\
&= \sum_{uv} [(\mathbf{T}_t \mathbf{J} \mathbf{T}_{kr})^T \odot \mathbf{M}_k \odot \mathbf{M}_k]_{uv}. \tag{92}
\end{aligned}$$

Thus, we obtain

$$\begin{aligned}
& \frac{\sum_{ij} [\mathbf{T}_{kr}(\mathbf{M}_k \odot \mathbf{M}_k)\mathbf{T}_t]_{ij}}{\partial \mathbf{M}_k} \\
&= (\mathbf{T}_t \mathbf{J} \mathbf{T}_{kr})^T \odot \mathbf{M}_k. \tag{93}
\end{aligned}$$

Furthermore,

$$\begin{aligned}
& \frac{\partial \sum_{ij} [\Phi_k]_{ij} \log \mathbf{e}_i^H (\mathbf{T}_{kr}(\mathbf{M}_k \odot \mathbf{M}_k)\mathbf{T}_t + \mathbf{O}_{kr} \mathbf{N} \mathbf{O}_t) \mathbf{e}_j}{\partial [\mathbf{M}_k]_{uv}} \\
&= \sum_{ij} \frac{[\Phi_k]_{ij}}{\mathbf{e}_i^H (\mathbf{T}_{kr}(\mathbf{M}_k \odot \mathbf{M}_k)\mathbf{T}_t + \mathbf{O}_{kr} \mathbf{N} \mathbf{O}_t) \mathbf{e}_j} \mathbf{e}_i^H \mathbf{T}_{kr} \mathbf{e}_u \mathbf{e}_v^H \mathbf{T}_t \mathbf{e}_j [\mathbf{M}_k]_{uv} \\
&= \mathbf{e}_v^H \mathbf{T}_t \sum_{ij} \mathbf{e}_j \frac{[\Phi_k]_{ij}}{\mathbf{e}_i^H (\mathbf{T}_{kr}(\mathbf{M}_k \odot \mathbf{M}_k)\mathbf{T}_t + \mathbf{O}_{kr} \mathbf{N} \mathbf{O}_t) \mathbf{e}_j} \mathbf{e}_i^H \mathbf{T}_{kr} \mathbf{e}_u [\mathbf{M}_k]_{uv}. \tag{94}
\end{aligned}$$

By defining $[\mathbf{Q}]_{ij} = \frac{[\Phi_k]_{ij}}{\mathbf{e}_i^H (\mathbf{T}_{kr}(\mathbf{M}_k \odot \mathbf{M}_k)\mathbf{T}_t + \mathbf{O}_{kr} \mathbf{N} \mathbf{O}_t) \mathbf{e}_j}$, we then obtain

$$\begin{aligned}
& \frac{\partial \sum_{ij} [\Phi_k]_{ij} \log \mathbf{e}_i^H (\mathbf{T}_{kr}(\mathbf{M}_k \odot \mathbf{M}_k)\mathbf{T}_t + \mathbf{O}_{kr} \mathbf{N} \mathbf{O}_t) \mathbf{e}_j}{\partial [\mathbf{M}_k]_{uv}} \\
&= \mathbf{e}_v^H \mathbf{T}_t \sum_{ij} \mathbf{e}_j [\mathbf{Q}]_{ij} \mathbf{e}_i^H \mathbf{T}_{kr} \mathbf{e}_u [\mathbf{M}_k]_{uv} \\
&= \mathbf{e}_v^H \mathbf{T}_t \mathbf{Q}^T \mathbf{T}_{kr} \mathbf{e}_u [\mathbf{M}_k]_{uv}. \tag{95}
\end{aligned}$$

Thus, we obtain

$$\begin{aligned}
& \frac{\partial \sum_{ij} [\Phi_k]_{ij} \log \mathbf{e}_i^H (\mathbf{T}_{kr}(\mathbf{M}_k \odot \mathbf{M}_k)\mathbf{T}_t + \mathbf{O}_{kr} \mathbf{N} \mathbf{O}_t) \mathbf{e}_j}{\partial \mathbf{M}_k} \\
&= (\mathbf{T}_t \mathbf{Q}^T \mathbf{T}_{kr})^T \odot \mathbf{M}_k. \tag{96}
\end{aligned}$$

REFERENCES

- [1] T. L. Marzetta, E. G. Larsson, H. Yang, and H. Q. Ngo, *Fundamentals of Massive MIMO*. Cambridge University Press, 2016.
- [2] E. Björnson, J. Hoydis, M. Kountouris, and M. Debbah, “Massive MIMO systems with non-ideal hardware: Energy efficiency, estimation, and capacity limits,” *IEEE Trans. Inf. Theory*, vol. 60, no. 11, pp. 7112–7139, 2014.
- [3] L. Lu, G. Y. Li, A. L. Swindlehurst, A. Ashikhmin, and R. Zhang, “An overview of massive MIMO: Benefits and challenges,” *IEEE J. Sel. Topics Signal Process.*, vol. 8, no. 5, pp. 742–758, 2014.
- [4] B. Clerckx, H. Joudeh, C. Hao, M. Dai, and B. Rassouli, “Rate splitting for MIMO wireless networks: a promising PHY-layer strategy for LTE evolution,” *IEEE Commun. Mag.*, vol. 54, no. 5, pp. 98–105, 2016.
- [5] Y. Zeng, R. Zhang, and T. J. Lim, “Wireless communications with unmanned aerial vehicles: opportunities and challenges,” *IEEE Commun. Mag.*, vol. 54, no. 5, pp. 36–42, 2016.
- [6] P. Chandhar, D. Danev, and E. G. Larsson, “Massive MIMO for communications with drone swarms,” *IEEE Trans. Wireless Commun.*, vol. 17, no. 3, pp. 1604–1629, 2018.
- [7] L. Liu and W. Yu, “Massive connectivity with massive MIMO—Part I: Device activity detection and channel estimation,” *IEEE Trans. Signal Process.*, vol. 66, no. 11, pp. 2933–2946, 2018.
- [8] A. Goldsmith, S. A. Jafar, N. Jindal, and S. Vishwanath, “Capacity limits of MIMO channels,” *IEEE J. Sel. Areas Commun.*, vol. 21, no. 5, pp. 684–702, 2003.
- [9] C. B. Peel, B. M. Hochwald, and A. L. Swindlehurst, “A vector-perturbation technique for near-capacity multi-antenna multiuser communication—part I: channel inversion and regularization,” *IEEE Trans. Commun.*, vol. 53, no. 1, pp. 195–202, 2005.
- [10] H. Weingarten, Y. Steinberg, and S. S. Shamai, “The capacity region of the Gaussian multiple-input multiple-output broadcast channel,” *IEEE Trans. Inf. Theory*, vol. 52, no. 9, pp. 3936–3964, 2006.
- [11] M. Sadek, A. Tarighat, and A. H. Sayed, “A leakage-based precoding scheme for downlink multi-user MIMO channels,” *IEEE Trans. Wireless Commun.*, vol. 6, no. 5, 2007.
- [12] D. Gesbert, M. Kountouris, R. W. Heath, C.-B. Chae, and T. Salzer, “From single user to multiuser communications: Shifting the MIMO paradigm,” *IEEE Signal Process. Mag.*, vol. 24, no. 5, pp. 36–46, 2007.
- [13] S. S. Christensen, R. Agarwal, E. De Carvalho, and J. M. Cioffi, “Weighted sum-rate maximization using weighted MMSE for MIMO-BC beamforming design,” *IEEE Trans. Wireless Commun.*, vol. 7, no. 12, pp. 4792–4799, 2008.
- [14] G. Caire, N. Jindal, M. Kobayashi, and N. Ravindran, “Multiuser MIMO achievable rates with downlink training and channel state feedback,” *IEEE Trans. Inf. Theory*, vol. 56, no. 6, pp. 2845–2866, 2010.
- [15] Q. Shi, M. Razaviyayn, Z.-Q. Luo, and C. He, “An iteratively weighted MMSE approach to distributed sum-utility maximization for a MIMO interfering broadcast channel,” *IEEE Trans. Signal Process.*, vol. 59, no. 9, pp. 4331–4340, 2011.
- [16] H. Q. Ngo, E. G. Larsson, and T. L. Marzetta, “Energy and spectral efficiency of very large multiuser MIMO systems,” *IEEE Trans. Commun.*, vol. 61, no. 4, pp. 1436–1449, 2013.
- [17] A. Adhikary, J. Nam, J.-Y. Ahn, and G. Caire, “Joint spatial division and multiplexing—the large-scale array regime,” *IEEE Trans. Inf. Theory*, vol. 10, no. 59, pp. 6441–6463, 2013.
- [18] C. Sun, X. Q. Gao, S. Jin, M. Matthaiou, Z. Ding, and C. Xiao, “Beam division multiple access transmission for massive MIMO communications,” *IEEE Trans. Commun.*, vol. 63, no. 6, pp. 2170 – 2184, 2015.
- [19] J. Wang and L. Dai, “Asymptotic rate analysis of downlink multi-user systems with co-located and distributed antennas,” *IEEE Trans. Wireless Commun.*, vol. 14, no. 6, pp. 3046–3058, 2015.

- [20] J. Park and B. Clerckx, “Multi-user linear precoding for multi-polarized massive MIMO system under imperfect CSIT,” *IEEE Trans. Wireless Commun.*, vol. 14, no. 5, pp. 2532–2547, 2015.
- [21] A. Liu and V. K. Lau, “Two-stage constant-envelope precoding for low-cost massive MIMO systems,” *IEEE Trans. Signal Process.*, vol. 64, no. 2, pp. 485–494, 2016.
- [22] M. Pei, J. Wei, K.-K. Wong, and X. Wang, “Masked beamforming for multiuser MIMO wiretap channels with imperfect CSI,” *IEEE Trans. Wireless Commun.*, vol. 11, no. 2, pp. 544–549, 2012.
- [23] O. Raeesi, A. Gokceoglu, Y. Zou, E. Björnson, and M. Valkama, “Performance analysis of multi-user massive MIMO downlink under channel non-reciprocity and imperfect CSI,” *IEEE Trans. Commun.*, vol. 66, no. 6, pp. 2456–2471, 2018.
- [24] B. Mondal and R. W. Heath Jr, “Channel adaptive quantization for limited feedback MIMO beamforming systems,” *IEEE Trans. Signal Process.*, vol. 54, no. 12, pp. 4717–4729, 2006.
- [25] M. K. Member and G. Caire, “Joint beamforming and scheduling for a multi-antenna downlink with imperfect transmitter channel knowledge,” *IEEE J. Sel. Areas Commun.*, vol. 25, no. 7, pp. 1468–1477, 2007.
- [26] K. Mamat and W. Santipach, “On optimizing feedback interval for temporally correlated MIMO channels with transmit beamforming and finite-rate feedback,” *IEEE Trans. Commun.*, vol. 66, no. 8, pp. 3407–3419, 2018.
- [27] A.-A. Lu, X. Gao, W. Zhong, C. Xiao, and X. Meng, “Robust transmission for massive MIMO downlink with imperfect CSI,” *IEEE Trans. Commun.*, vol. 67, no. 8, pp. 5362 – 5376, 2019.
- [28] A. M. Sayeed, “Deconstructing multi-antenna fading channels,” *IEEE Trans. Signal Process.*, vol. 50, no. 10, pp. 2563–2579, 2002.
- [29] W. Weichselberger, M. Herdin, H. Ozelcik, and E. Bonek, “A stochastic MIMO channel model with joint correlation of both link ends,” *IEEE Trans. Wireless Commun.*, vol. 5, no. 1, pp. 90–100, 2006.
- [30] X. Gao, B. Jiang, X. Li, A. B. Gershman, and M. R. McKay, “Statistical eigenmode transmission over jointly correlated MIMO channels,” *IEEE Trans. Inf. Theory*, vol. 55, no. 8, pp. 3735–3750, 2009.
- [31] L. You, X. Q. Gao, X.-G. Xia, N. Ma, and Y. Peng, “Pilot reuse for massive MIMO transmission over spatially correlated Rayleigh fading channels,” *IEEE Trans. Wireless Commun.*, vol. 14, no. 6, pp. 3352 – 3366, 2015.
- [32] S.-i. Amari, *Information Geometry and Its Applications*. Springer, 2016.
- [33] K. B. Petersen and M. S. Pedersen, “The matrix cookbook,” *Technical University of Denmark*, pp. 7–7, 2006.
- [34] P.-A. Absil, R. Mahony, and R. Sepulchre, *Optimization Algorithms on Matrix Manifolds*. Princeton University Press, 2009.
- [35] R. Couillet and M. Debbah, *Random Matrix Methods for Wireless Communications*. Cambridge University Press, 2011.
- [36] W. Hachem, O. Khorunzhiy, P. Loubaton, J. Najim, and L. Pastur, “A new approach for mutual information analysis of large dimensional multi-antenna channels,” *IEEE Trans. Inf. Theory*, vol. 54, no. 9, pp. 3987–4004, 2008.
- [37] R. Couillet, M. Debbah, and J. W. Silverstein, “A deterministic equivalent for the analysis of correlated MIMO multiple access channels,” *IEEE Trans. Inf. Theory*, vol. 57, no. 6, pp. 3493–3514, 2011.
- [38] C.-K. Wen, G. Pan, K.-K. Wong, M. Guo, and J.-C. Chen, “A deterministic equivalent for the analysis of non-Gaussian correlated MIMO multiple access channels,” *IEEE Trans. Inf. Theory*, vol. 59, no. 1, pp. 329–352, 2013.
- [39] A.-A. Lu, X. Gao, and C. Xiao, “Free deterministic equivalents for the analysis of MIMO multiple access channel,” *IEEE Trans. Inf. Theory*, vol. 62, no. 8, pp. 4604–4629, 2016.
- [40] J. A. Mingo and R. Speicher, “Operator-valued free probability theory and block random matrices,” in *Free Probability and Random Matrices*. Springer, 2017, pp. 225–247.
- [41] S. Jaeckel, L. Raschkowski, K. Börner, and L. Thiele, “Quadriga: A 3-D multi-cell channel model with time evolution for enabling virtual field trials,” *IEEE Trans. Antennas Propag.*, vol. 62, no. 6, pp. 3242–3256, 2014.